Manufacturing Technologies and Applications MATECA



Experimental Investigation of Machinability of AISI 316L Stainless Steel by High Feed Milling Method

Yusuf Siyambaş^{1,*} D, Aslan Akdulum²

¹Erzincan Binali Yıldırım University Vocational High School, Department of Machinery and Metal Technologies, Erzincan, Turkey ²Hacettepe University Başkent OSB Vocational School of Technical Sciences, Department of Machinery and Metal Technologies, Ankara, Turkey

ABSTRACT

This study aims to investigate the effects of different cutting conditions on the machining performance of difficult-to-machine AISI 316L stainless steel using the high-feed milling method. Experiments were conducted using different spindle speeds and feed rates; cutting temperatures were recorded using a thermal camera, surface roughness measured with a profilometer, and tool wear examined via SEM and EDS analysis. The findings reveal that air-assisted cooling reduced the maximum cutting temperature from 321°C to 197°C (a 39% reduction) compared to dry cutting. In terms of surface roughness, the lowest Ra value achieved under air-assisted conditions was 0.929 μ m, compared to 1.100 μ m under dry conditions. Tool wear analyses showed that air-assisted cooling significantly reduced coating delamination and material adhesion on the tool surface. These advantages provided by the air-assisted system stand out as an environmentally friendly and energy-efficient alternative, especially in processes where high temperatures and tool wear are critical.

Keywords: AISI 316L, High feed milling, Sustainable machining, Surface roughness, Cutting temperature, Tool wear

AISI 316L Paslanmaz Çeliğin Yüksek İlerlemeli Frezeleme Yöntemiyle İşlenebilirliğinin Deneysel Araştırılması

ÖZET

Bu çalışma, işlenmesi güç olan AISI 316L paslanmaz çeliğin yüksek ilerlemeli frezeleme yöntemiyle işlenmesinde farklı kesme koşullarının işleme performansı üzerindeki etkilerini incelemeyi amaçlamaktadır. Deneyler farklı iş mili devir sayıları ve ilerleme hızlarında gerçekleştirilmiş; kesme sıcaklıkları termal kamera ile, yüzey pürüzlülüğü profilometre ile ölçülmüş ve takım aşınmaları SEM ile EDS analizleriyle incelenmiştir. Bulgular, hava destekli soğutmanın kesme bölgesindeki maksimum sıcaklığı 321°C'den 197°C'ye (%39 azalma) düşürdüğünü göstermektedir. Yüzey pürüzlülüğü açısından, hava destekli sistemde elde edilen en düşük Ra değeri 0.929 µm, kuru işlemede ise 1,100 µm olarak ölçülmüştür. Takım aşınması analizleri, hava destekli kesimlerde kaplama tabakasında oluşan hasarların ve malzeme yapışmalarının önemli ölçüde azaldığını ortaya koymuştur. Bu bulgular, hava destekli sistemin çevreci ve enerji verimli bir alternatif olarak, yüksek sıcaklıkların ve takım aşınmasının kritik olduğu uygulamalarda öne çıktığını göstermektedir.

Anahtar Kelimeler: AISI 316L, Yüksek ilerlemeli frezeleme, Sürdürülebilir işleme, Yüzey pürüzlülüğü, kesme Sıcaklığı, Takım aşınması

1. INTRODUCTION

In machining processes, the cutting parameters, such as depth of cut (Doc), speed (n), and feed rate (f), are the basic variables that directly affect the cutting mechanism [1]. The proper selection of these parameters plays a crucial role in determining outputs such as temperature, chip formation, surface integrity, and tool life during cutting. Especially in high-strength and difficult-to-machine materials, determining the appropriate cutting conditions is crucial for improving surface quality and minimizing tool wear. In milling operations, various influencing factors such as tool runout, tool deflection caused by cutting forces [2], or vibration [3] affect the workpiece surface topography [4]. In order to eliminate these negativities, studies have been carried out in recent years to improve the surface quality of workpieces through high-feed milling (HFM) processes [5]. High- feed milling stands out as an effective method for machining free-form surfaces thanks to its

^{*}Corresponding author, e-mail: yusuf.siyambas@erzincan.edu.tr

combination of small-diameter tools and high material removal rates and is widely preferred in machinability studies [4].

Stainless steels are widely preferred in many areas, especially in the defense industry, chemical industry, food industry, and medical applications, due to their superior properties such as high mechanical strength, excellent corrosion resistance, and biocompatibility [6,7]. AISI 316L stainless steel, one of the prominent subtypes of this material group, has a structure with increased weldability and reduced grain boundary carburization thanks to its low carbon content [8]. Its high corrosion resistance, especially in marine environments and aggressive chemical environments, distinguishes it from other types of stainless steel [9,10]. However, the properties of this steel, such as high ductility, strength, and low thermal conductivity, create serious difficulties in terms of machinability; accelerate tool wear; and cause high temperatures in the cutting zone [11]. This situation leads to decreased surface quality and shortened tool life in machining processes. In this context, controlling the temperature in the cutting zone and implementing an effective cooling strategy are of critical importance in terms of both improving surface quality and extending tool life. Traditional cooling methods do not align with sustainable production goals due to their environmental impacts and high operating costs. For this reason, air-assisted cooling systems, which are among the environmentally friendly and energy-efficient alternative solutions, are among the applications that have attracted attention in recent years [12].

There are many studies on high feed milling in the literature. In an experimental study, surface roughness and force values were investigated in HFM of vermicular cast iron with different hardness, and successful predictions were obtained with artificial neural networks (ANN). Best results were obtained at high hardness, low feed, and high cutting speed [13]. In another experimental study, a model was developed to predict the cutting forces in HFM of AISI P20 steel. The model was found to be successful, especially at high depths of cut, and it was stated that the horizontal insert provided an advantage in wear balance [14]. In another study, conventional and high feed milling methods were compared in the machining of AlZn5.5MgCu aluminum alloy. The study revealed that high feed milling is more time efficient [15]. In another study, the relationship between insert damage and surface roughness in high-speed milling of 17-4 PH stainless steel was investigated, and fatigue fracture was detected at low speeds, and notch wear was detected at high speeds. The effect of damage on surface quality is emphasized [16]. Another study indicated that flank wear was the dominant wear type in HFM of X38CrMoV53 steel, and excessive wear caused insert fracture. The highest material removal rate occurred at low feed rate and high depth of cut [17]. In another study, the effects of cutter and wiper inserts on tool life, wear, and surface quality in Ti-6Al-4V alloy were investigated in HFM in a dry environment, and it was reported that the surface roughness remained between 0.7 µm and there was a 5-8% increase in microhardness [18]. In another study, conventional and high feed milling (HFM) of CK45 steel were compared, and it was found that HFM reduces machining time and is suitable for roughing but may adversely affect surface quality on vertical surfaces [19]. In another study, the effect of different cutting parameters on the cutting forces in the HFM process of Ti-6Al-4V titanium alloy with square and triangular inserts was investigated. The results show that feed per tooth and axial depth of cut increase the cutting force; insert geometry and cutting temperature also affect the cutting force and tool life [20]. In another study, the effects of different chipbreaker geometries on surface roughness and cutting forces in face milling of AISI 1040 steel were investigated. While increasing feed rate increased surface roughness and cutting forces, increasing cutting speed decreased these values. Significant effects of the cutting-edge geometry on the surface quality were observed [21].

In the literature, many experimental studies have been conducted on high feed milling (HFM) in different materials and cutting conditions. The effects of HFM on cutting forces, surface roughness, tool wear, and tool life were investigated in a variety of materials, from vermicular cast iron to titanium alloys and from stainless and hardened steels to aluminum alloys. In general, it was found that high feed rates increased the cutting forces and surface roughness, but cutting speed and tool geometry positively affected the performance. While it is emphasized that HFM significantly reduces machining time and is particularly suitable for rough machining, it is also stated that it has limitations in terms of surface quality in some cases. In addition, the accuracy of cutting force and wear predictions has been increased with advanced modeling methods, and it has been reported that surface quality can be maintained even under uncooled process conditions. These studies demonstrate the potential of HFM as a sustainable and efficient processing strategy in different materials and parameters.

Although air-assisted cooling has been studied in various machining contexts, the current study offers a unique contribution by combining this environmentally friendly method with HFM of AISI 316L stainless steel—a material known for its poor machinability. Unlike previous studies, which predominantly focus on conventional milling methods or other material types, this research specifically investigates the effects of air-assisted cooling on cutting temperature, surface roughness, and tool wear in HFM of AISI 316L. The study

not only provides experimental evidence on the thermal and mechanical benefits of air-assisted cooling but also highlights its potential as a sustainable and effective alternative in the machining of difficult-to-cut materials. This novel combination of cutting strategy and cooling technique distinguishes the current work within the field of sustainable machining.

In this work, the influences of dry and air-assisted cutting conditions on cutting temperature (T), surface roughness (Ra), and cutting tool wear during the machining of AISI 316L stainless steel by the HFM method were experimentally investigated. The main purpose of the study is to reveal the technical advantages that air-assisted cooling, an environmentally friendly method, can provide in the milling process of a difficult-to-machine material such as AISI 316L. The findings show that this method can make significant contributions to industrial applications with its potential to not only reduce cutting temperatures but also improve surface quality and limit tool wear.

2. MATERIAL AND METHOD

The setup prepared for the surface milling operation of the AISI 316L workpiece with a high-feed tool under dry and air-cooling conditions is shown in Figure 1 and Figure 2.



Figure 1. Experimental setup prepared for surface milling.

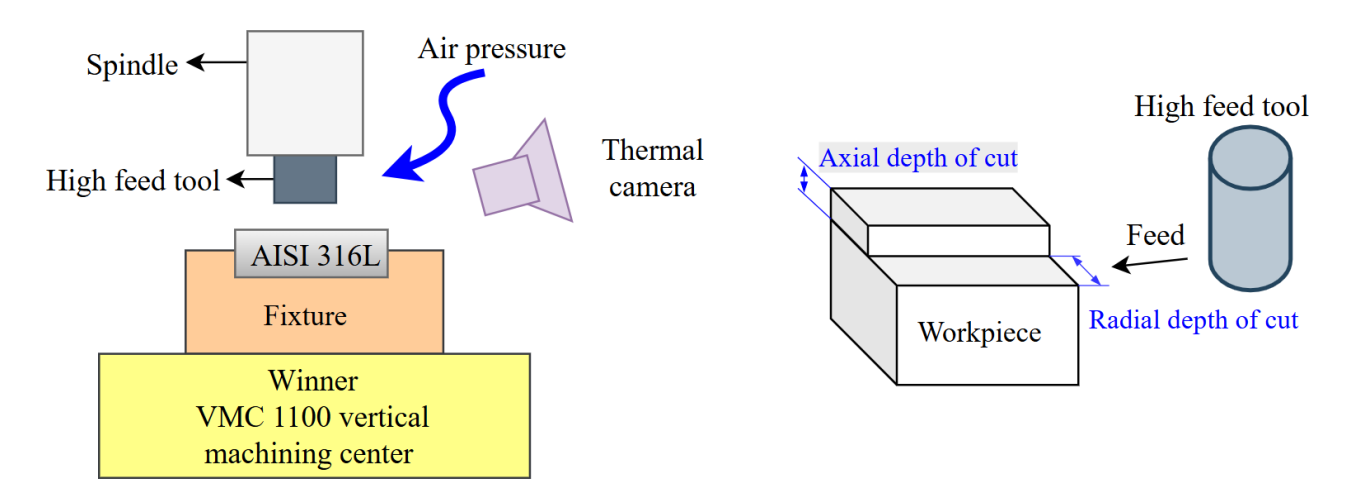


Figure 2. Schematic of experimental setup and cutting parameters.

AISI 316L austenitic stainless steel was prepared in 30×45×10 mm dimensions and used in the experiments. Workpieces are supplied in accordance with the ASTM A240 standard [22]. The chemical composition and mechanical properties of AISI 316L austenitic stainless steel are given in Table 1. Milling experiments were conducted on a Winner VMC 1100 brand vertical machining center with a maximum spindle speed of 8000 rpm and a spindle motor of 7.5 kW. The machine tool has a Mitsubishi M80 control panel. No coolant was used in dry experiments. Air cooling conditions were achieved with a system with an outlet pressure of approximately 6 bar integrated into the machine tool.

Table 1. Chemical composition and mechanical properties of AISI 316

Chemical composition										
Element	C	Mn	S	P	Si	Ni	Cr	N	Mo	Fe
% by wt	0.02	0.8	0.004	0.04	0.28	12.07	16.58	0.035	2.02	Bal.
Mechanical properties										
Density (g/cm ³)			8							
Young's modulus (GPa)			193							
Tensile strength (MPa)			660							
Yield strength (MPa)			320							
Elongation (%)			55							
Hardness (HRB)				79						

The cutting insert brand used in the experimental study is Korloy, the cutter geometry is LNMX 060310R-MM, and the cutter quality is PC5400. The cutting tip has a PVD AlCrN (AlCiN) coating. New inserts were installed in each experiment. The high-feed tool used has 5 cutting edges, and the cutter diameter is 32 mm. For the face milling operation, the cutting depth was taken as a constant 0.5 mm. Surface milling experiments were carried out using the parameters in Table 2 according to the full factorial test principle. A total of 18 experiments were carried out, 9 each under dry and air cooling conditions. A cutting tool with a diameter of 32 mm was employed in the experiments. The spindle speeds were set at 1000, 1500, and 2250 rpm, corresponding to cutting speeds of approximately 100.5 m/min, 150.8 m/min, and 226.2 m/min, respectively. Based on the selected spindle speeds and the number of cutting edges, feed rates of 0.178, 0.267, 0.4, 0.6, and 0.9 mm/rev were considered during the machining process.

Table 2. Face milling operation parameters.

Face milling parameters									
Spindle speed	Feed rate	Cutting	Axial depth of cut	Radial depth of cut mm					
Rpm	mm/min	environments	mm						
1000	2000	Derv							
1500	3000	Dry	0.5	20					
2250	4500	Air							

The cutting environment was recorded in real time using a FLIR brand thermal camera. The images were then examined frame by frame to obtain average cutting temperatures. The average temperature values were determined by focusing on the region closest to the contact zone between the cutting tool and the workpiece. The thermal camera recorded images at a rate of 30 frames per second. All recordings captured during the cutting process were examined frame by frame. The cutting temperature was then calculated by averaging all the temperature values obtained throughout the cutting operation. Scanning electron microscope (SEM) images were taken with a Hitachi High-Tech SU8700 device. A Mitutoyo SJ-210 brand device was used for surface roughness measurements. Surface roughness values were calculated by averaging three measurements taken from four edges of the milled surface.

3. EXPERIMENTAL RESULTS AND DISCUSSION

3.1. Investigation of Cutting Temperature

Figure 3 presents the comparative effects of dry and air-assisted cutting conditions applied at different feed rates (2000–4500 mm/min) and speeds (1000–2250 rpm) on the cutting temperature in the HFM process of AISI 316L stainless steel. In general, the cutting temperatures achieved under dry machining conditions were significantly higher compared to air-assisted machining for all cutting parameter combinations. This situation shows that the temperature accumulation increases due to the inability to remove the heat accumulated in the cutting zone in dry machining, and cooling cannot be provided by evaporation or convection.

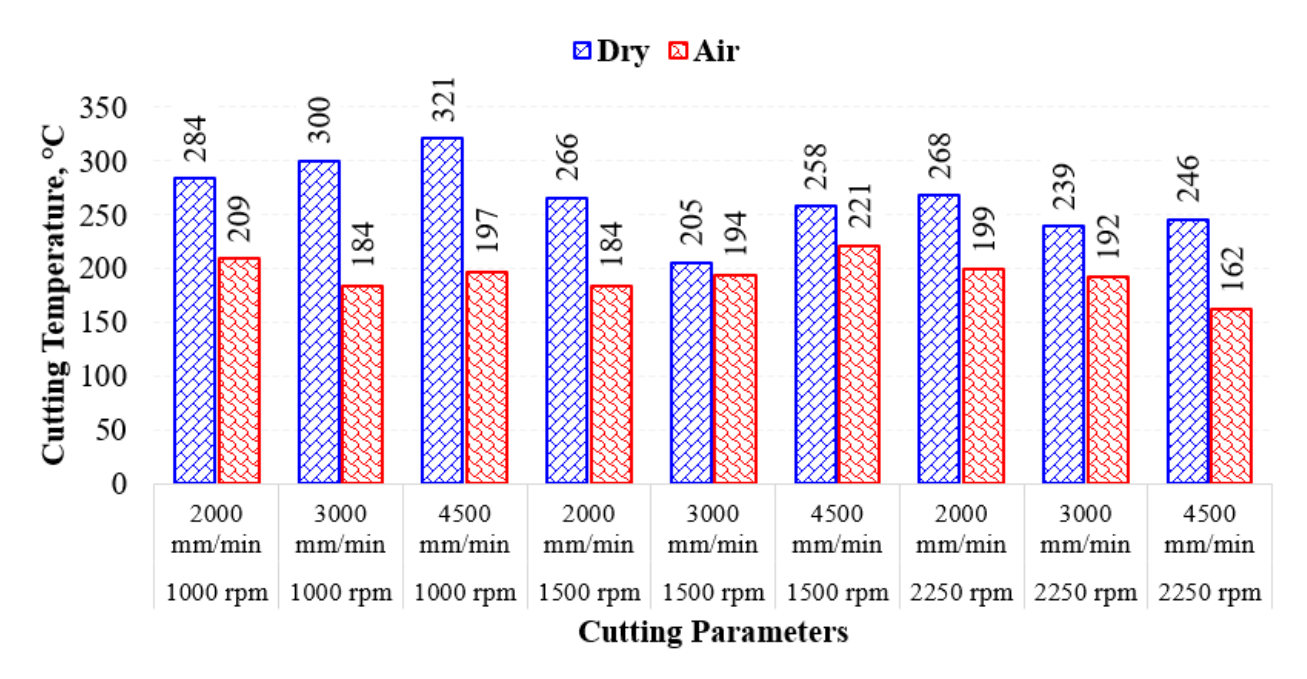


Figure 3. Effect of dry and air conditions on cutting temperature.

The highest cutting temperature was recorded as 321°C at 1000 rpm and 4500 mm/min feed rate under dry machining. In these conditions, despite the increase in cutting energy due to the high feed rate, the low speed caused the chip to remain in the machining zone for a longer time and increased heat accumulation. [23]. Under the same cutting parameters, the temperature dropped to 197°C in the air-assisted process, a reduction of approximately 39%. Similarly, the temperature values remained in the range of 162-221°C in air-assisted mode under all process milling conditions, indicating that the airflow provided an effective heat removal mechanism in the cutting zone. The increase in speed (from 1000 to 2250 rpm) did not reduce the temperatures in absolute terms, but when evaluated together with the feed rate, it created a more balanced effect in terms of thermal load distribution. For example, while the dry process temperature was 239°C at 2250 rpm and a 3000 mm/min feed rate, this value was recorded as 192°C in the air-assisted process. These values show that increasing cutting speeds and effective chip removal can provide thermal balance, and the air-assisted system is an advantageous complementary element at this point [24]. As a result, air-assisted cooling suppressed the high heat accumulation tendency of AISI 316L, significantly reducing cutting temperatures and positively affecting machining performance. The findings reveal that air-assisted cooling may be more advantageous than dry processing, especially in applications where high feed rates are used. Failure to effectively remove the heat accumulated in the cutting zone during dry machining may lead to negative consequences such as tool wear, workpiece deformation, and deterioration of surface quality [25]. Air-assisted cooling provides a more balanced thermal environment by transferring heat away from the cutting zone, especially in materials with low thermal conductivity such as AISI 316L.

The feed rates were increased in steps of 50% in order to reveal more clearly the effects on the cutting temperature; however, the temperature trends obtained under dry machining conditions did not always show a linear or unidirectional behavior. This can be explained by non-linear interactions between feed rate, spindle speed, and material response. This effect is particularly more pronounced in the machining of AISI 316L stainless steel, which is characterized by low thermal conductivity and a high tendency for work hardening. At high feed rates, thermal saturation may occur as the heat-carrying capacity of the chip reaches its limit.

Additionally, increased friction in the tool—chip contact area, changes within the shear zone, and the system's thermal inertia may lead to unexpected local temperature peaks or stabilizations.

Figures 4a and 4b show the changes in the cutting temperatures during surface milling of AISI 316L stainless steel under dry and air-assisted cutting conditions, respectively, depending on the feed rate and rotational speed parameters, with three-dimensional surface graphics. It is clearly seen from both graphs that the cutting temperature is sensitive to changes in both feed rate (FR) and spindle speed (SS); however, the magnitude and distribution of this change vary significantly depending on the cooling condition used. In Figure 4a, which represents the dry machining condition, the minimum cutting temperature was obtained at medium cutting parameters, while the maximum cutting temperature was obtained at minimum spindle speed and maximum feed rate. When looking at the overall surface, the temperature change shows sharper and more abrupt trends, suggesting that a more unstable thermal environment is formed during the dry process.

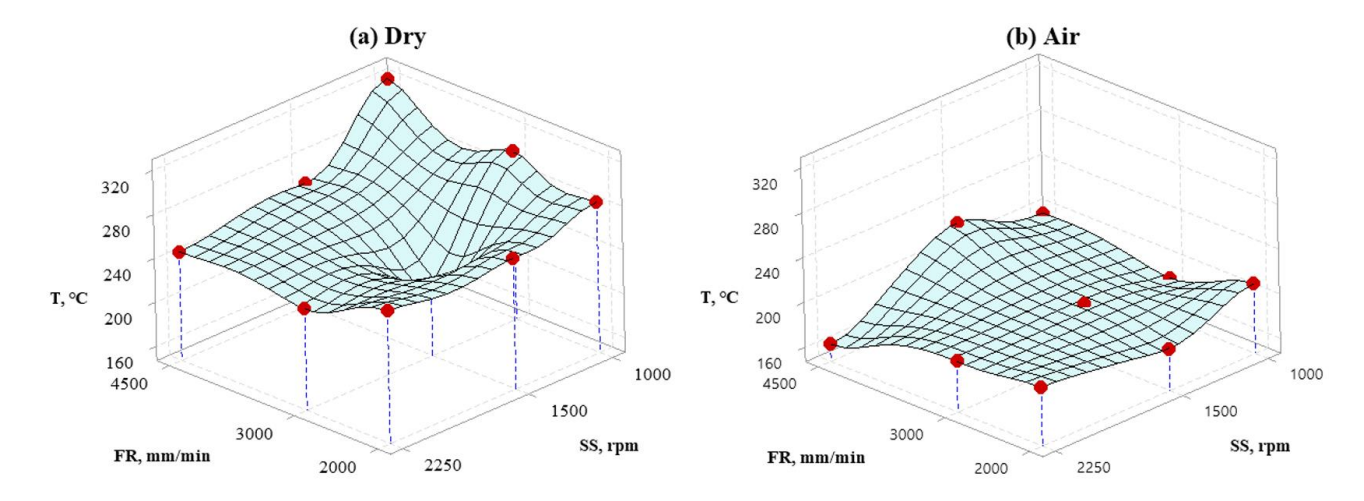


Figure 4. Changes in cutting temperatures depending on spindle speed and feed rate.

In Figure 4b, which shows the air-assisted cutting condition, the temperature distribution was in the lower ranges (162–221°C). Under air cooling conditions, the lowest cutting temperature was obtained at the maximum spindle speed and feed rate combination, while the highest cutting temperature was obtained at the maximum feed rate and medium spindle speed. Especially at low speeds and medium feed speeds, the observed temperature values remained limited. This reveals that the airflow can effectively remove heat from the cutting zone, thus providing a more stable thermal structure during the process [26]. Additionally, the smoother transitions in the air-assisted graph indicate that air blowing increases the controllability of the process by limiting temperature increases. In general comparison, it can be understood that the air-assisted cutting condition not only significantly reduces the cutting temperature but also makes the temperature distribution more stable and predictable. It shows that air-assisted applications offer significant advantages over dry processing in terms of cutting temperature.

3.2. Examination of Surface Roughness

The influences of dry and air mediums on Ra are given in Figure 5. When the surface roughness values obtained under different cutting parameters in both dry and air-assisted cutting conditions were compared, it was seen that air-assisted applications generally reached lower Ra values and thus had the potential to provide higher quality surfaces. Under dry cutting conditions, the highest surface roughness value of 1.654 µm was obtained at the combination of 1000 rpm and 4500 mm/min feed speed. This can be explained by the fact that low speed and high feed rate create a greater metal removal load on the tool [27]. Additionally, increased cutting temperature in dry conditions accelerates tool wear and increases surface deterioration [28]. However, the lowest Ra value in dry cutting was observed at 2250 rpm and 2000 mm/min parameters with 1100 µm. This can be attributed to the fact that high speed provides shorter contact time, facilitating the dissipation of heat in the cutting zone [29]. In air-supported conditions, the lowest surface roughness was obtained with 0.929 µm at 1000 rpm and 2000 mm/min parameters. This can be attributed to the fact that low cutting speed and air cooling together effectively reduce the heat and chip jamming in the cutting zone. However, the highest Ra value of 1.414 µm was observed in the air-supported system at 2250 rpm and 4500 mm/min conditions. This suggests that air support alone may not be sufficient in terms of surface roughness at high feed rates [30]. When both conditions are evaluated together, it is seen that the surface roughness values show a more balanced

distribution in air-assisted cutting, the Ra values remain in a narrower range, and the surface quality is generally improved.

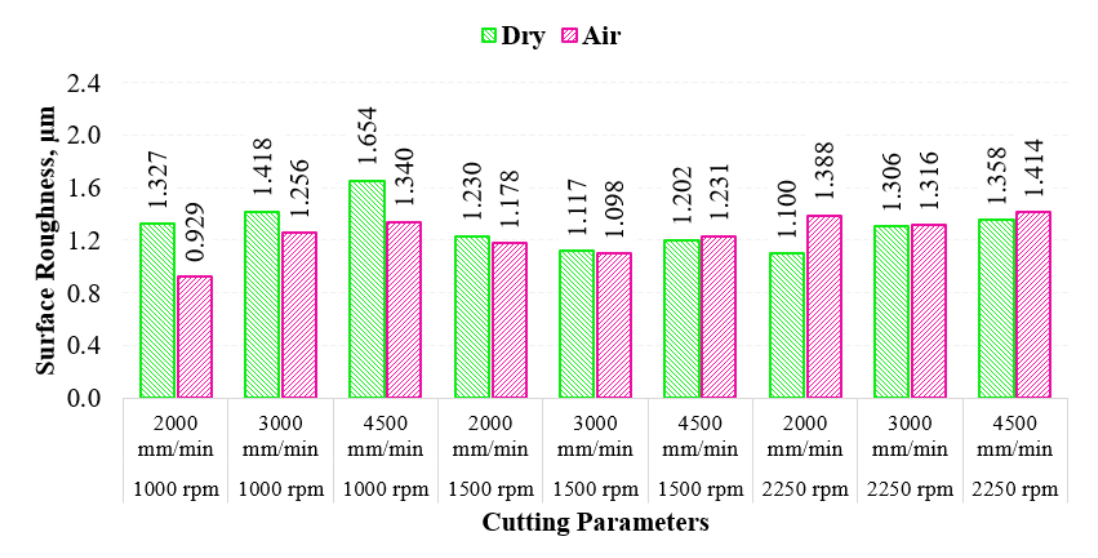


Figure 5. Effects of dry and air conditions on surface roughness.

Compared to dry machining, air-assisted conditions performed more effectively, especially at low and moderate feed rates, which was associated with reduced thermal and mechanical effects of machining. As a result, it has been shown that an air-assisted cutting environment is more advantageous than dry machining in terms of minimizing surface deterioration due to high temperatures and tool wear in applications aimed at improving surface quality.

In Figure 6, the effect of different cutting parameters on Ra during face milling of AISI 316L stainless steel is presented comparatively under dry and air-assisted cooling conditions. When dry cutting conditions were examined, the lowest Ra value was obtained in the combination of maximum SS (2250 rpm) and minimum FR (2000 mm/min). This result can be explained by the fact that high speed reduces the contact time in the cutting zone and provides a smoother cut.

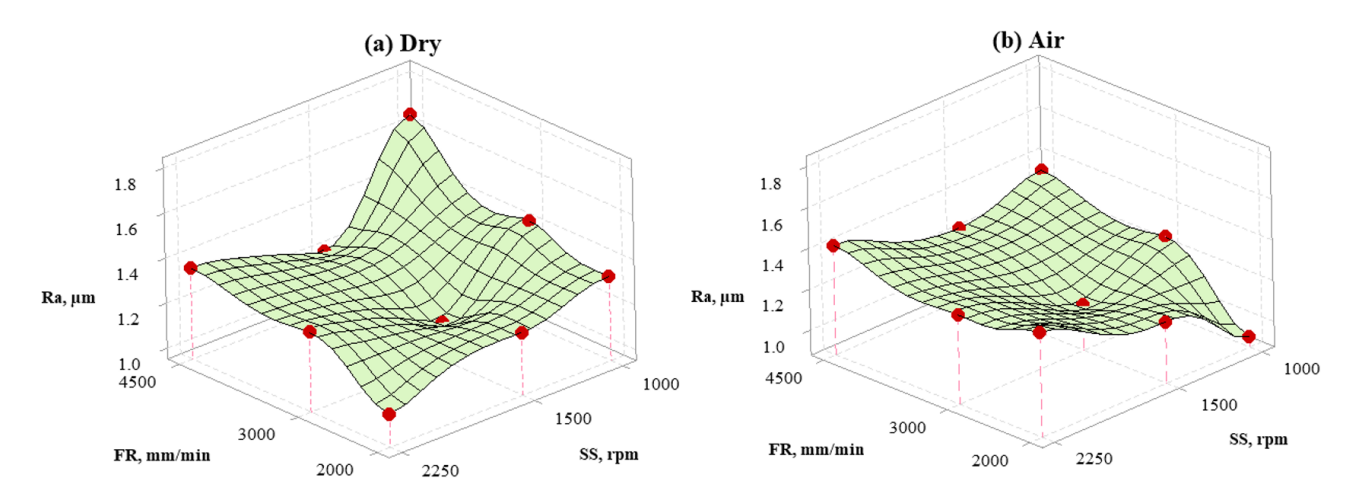


Figure 6. Change in surface roughness depending on spindle speed and feed rate.

On the other hand, the highest Ra value was observed under low SS (1000 rpm) and high FR (4500 mm/min) parameters, which is related to the fact that high feed rates increase the chip volume, accelerate tool wear, and cause irregularities on the surface. Under dry conditions, the increase of FR led to a significant increase in Ra, especially at low and high SS levels. However, lower Ra values were obtained with medium FR (3000 mm/min) under medium SS (1500 rpm) conditions. This situation can be explained by the more balanced distribution of thermal and mechanical loads in the cutting zone. In air-assisted cooling conditions, the lowest Ra value was obtained with the lowest SS and FR combination (1000 rpm–2000 mm/min). Under these

parameters, the airflow is evaluated to effectively reduce the temperature and chip jamming in the cutting zone, thus supporting the formation of a smoother surface. On the other hand, the highest Ra value occurred when both SS and FR were at their highest levels (2250 rpm–4500 mm/min). This indicates that the intense thermomechanical loads created by high cutting speeds and feed rates limit the effectiveness of air-assisted cooling. In general, Ra values ranged from 1.100 to 1.654 µm in dry machining conditions and from 0.929 to 1.414 µm in air-assisted conditions. This difference can be explained by the fact that air-assisted cooling limits the temperature increase in the cutting zone, slows down tool wear, and enables smoother chip formation [31]. As a result, it can be said that the air-assisted system causes more controlled and narrow-range changes in the surface roughness; therefore, it is more effective in improving the surface quality compared to dry cutting.

3.3. Examination of Inserts

Figure 7 describes the SEM images of the wear zones formed on the cutting tool surfaces used under dry (Figure 7a–c) and air-assisted cooling (Figure 7d–f) conditions during surface milling of AISI 316L stainless steel at 1500 rpm and 3000 mm/min cutting parameters and the EDS analysis results obtained from the relevant regions. These analyses are important for the characterization of wear mechanisms such as diffusion, adhesion, and coating loss that occur on the tool surface during the cutting process. Dry machining conditions (Figure 7a-c) were investigated in detail. In the SEM image shown in Figure 7a, significant accumulated chip and adhering workpiece material are observed at the tool tip under dry cutting conditions. There is significant material accumulation and coating damage, especially on the edge. EDS analyses of these regions were carried out at two different points, as shown in Figure 7a. In Figure 7b, the detection of high content of workpiece components such as Fe (48.5%), C (23.2%), Cr (12.8%), and Ni (6.8%) clearly reveals that the workpiece material adheres to the tool surface. In Figure 7c, especially the high W (41.9%) and C (35.1%) ratios indicate the tungsten carbide-based coating structure of the cutting tool. However, the presence of small amounts of Fe (5.8%) and Cr (1.8%) here also indicates that the workpiece material is transported to the coating surface by diffusion or adhesion. These findings reveal that the tool is exposed to high temperatures under dry cutting conditions; thus, diffusion and adhesion-type wear develop significantly [32]. When the air-assisted cooling conditions (Figure 7d-f) are examined, the SEM image in Figure 7d reveals a smoother and more regular tool surface in the air-assisted cooling environment. It is observed that the accumulated chips and adhesion effects are reduced, and the surface is relatively less damaged compared to dry conditions. EDS analyses performed in the relevant regions are presented in Figure 7e and Figure 7f. In Figure 7e, the density of elements belonging to the carbide structure, such as W (45.6%) and C (25.3%), is in the foreground. At the same time, the presence of certain levels of binder and coating elements such as Co (5.6%) and Cr (3.3%) shows that the coating layer is largely protected and minimum damage occurs on the tool surface. The presence of elements such as Fe (10.7%) and Ni (1.5%) in the workpiece at various levels indicates the existence of adhesion and diffusion. In Figure 7f, a more balanced composition is observed. The ratios of Fe (45.6%), Cr (12.1%), and Ni (6.7%) indicate a certain level of adhesion possibility.

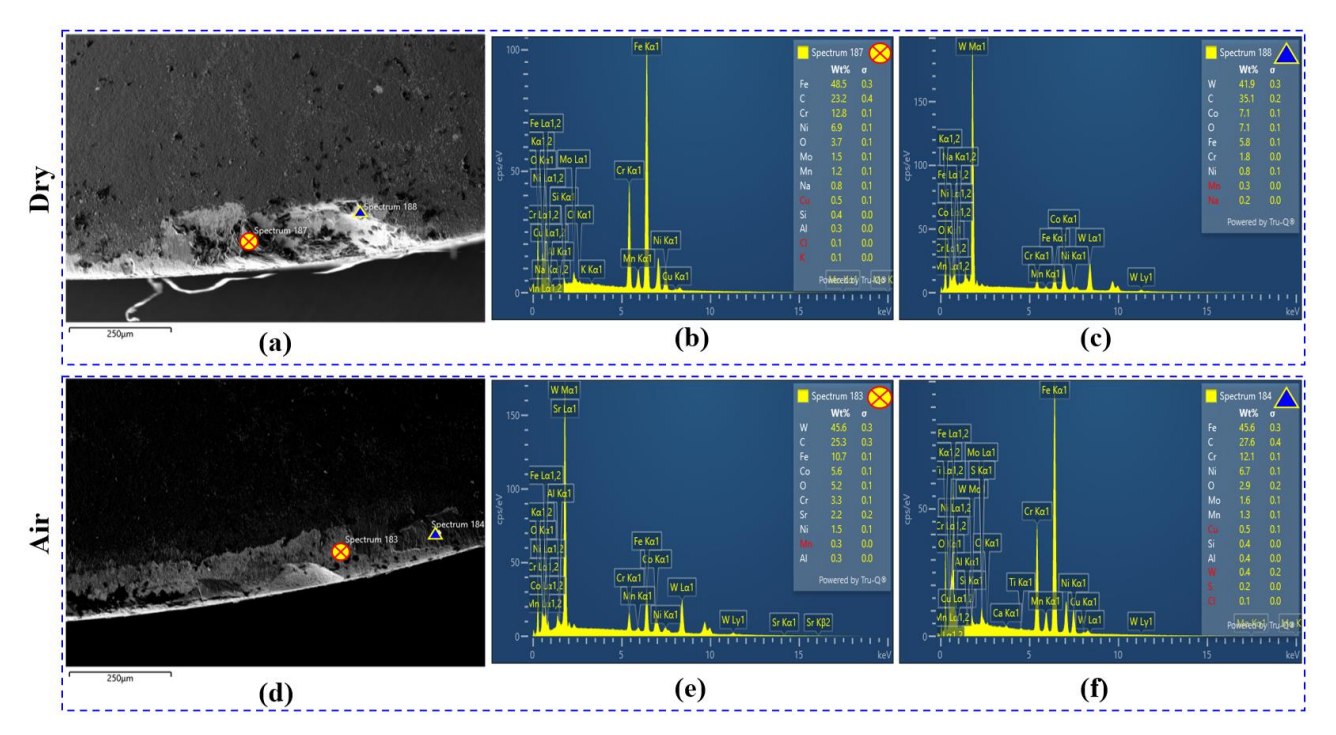


Figure 7. Electron images and element distribution for dry and air cooling conditions (1500 rpm ve 3000 mm/min).

W (0.4%) and C (27.6%) ratios indicate that the coating layer in this region is slightly eroded. In general, it has been observed that air-assisted cooling limits the thermal stresses that may occur on the cutting tool surface, thus preserving the coating integrity better and minimizing the adhesion of the workpiece material to the tool surface. SEM and EDS analyses revealed that the tool underwent more severe wear under dry machining conditions and that adhesion and diffusion mechanisms were particularly effective. On the other hand, air-assisted cooling reduced the thermal load on the tool surface, maintained the integrity of the coating, and significantly limited the wear effects. This shows that air cooling offers significant advantages in terms of surface quality and tool life.

Figure 8 presents the chemical changes that occur on the cutting tool surface during the machining of AISI 316L stainless steel at 2250 rpm and 4500 mm/min cutting parameters under dry (Figure 8a–c) and air-assisted cooling (Figure 8d–f) conditions, comparatively through SEM images and EDS analyses. These analyses provide important information in determining the deterioration of the tool coating layer and the workpiece material transfer. When dry cutting conditions (Figure 8a–c) are examined, it is observed in the SEM image in Figure 8a that the structural integrity of the tool surface is largely preserved, but there is material transfer and coating effect in local areas. The analysis results given in Figure 8b and Figure 8c, taken from two different points, support this situation. The EDS spectrum of Figure 7b is characterized by high C (65.1%) and Fe (4.6%) content. Figure 8c highlights the elements of the coating layer. Here, coating elements such as Al (22.4%) and Ti (25.8%) were detected intensively. This shows that the coating still exists in the analyzed area. These analyses show that during dry cutting, the coating can be preserved in some areas of the tool, but workpiece elements can be transported to the surface locally through adhesion and diffusion. When the air-assisted cooling conditions (Figure 8d–f) are examined, the SEM image shown in Figure 8d reveals that air-assisted cooling creates a more stable structure on the tool surface and wear develops in a localized manner.

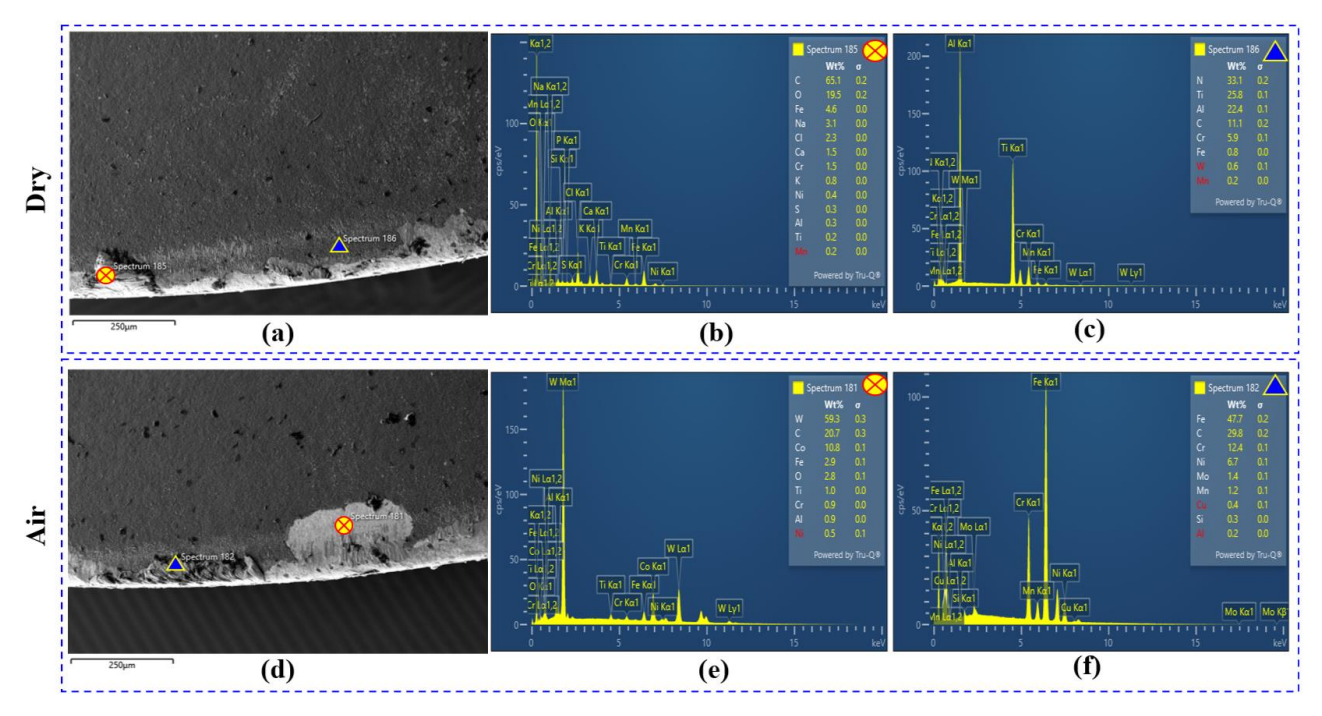


Figure 8. Electron images and element distribution for dry and air cooling conditions (2250 rpm ve 4500 mm/min).

Figure 8e and Figure 8f analyses taken from these regions are important in evaluating the effect of thermal and mechanical effects on the coating layer. Figure 8e shows the high density of coating elements such as W (59.3%) and Co (10.8%). It can be said that the coating layer has peeled off in this area. However, it is quite localized in terms of the area it covers. Figure 8f presents the chemical composition in a different region. At this point, the presence of elements specific to AISI 316L steel, such as Fe (47.7%), Cr (12.4%), and Ni (6.7%), indicates that the workpiece material is transferred to the tool surface to a limited extent. However, the presence of coating elements such as Mo (1.4%) and Mn (1.2%) indicates that this layer is also partially affected during adhesion. These findings suggest that air-assisted cooling effectively protects the coating surface but may occasionally cause limited adhesion of the workpiece material.

Figure 9 shows the SEM images (Figure 9a, c) and elemental distribution maps (Figure 9b, d) of the cutting edge surfaces obtained after the surface milling process performed at 1500 rpm and 3000 mm/min feed parameters. The images comparatively present the structural and chemical changes occurring on the tool surface in dry (Figure 9a-b) and air-assisted (Figure 9c-d) cutting conditions. When the SEM image in Figure 9a, which was formed under dry cutting conditions, is examined in detail, obvious morphological deteriorations, layer peelings, and dense deposits are observed, especially around the cutting edge. This type of surface damage can be associated with thermomechanical stresses and coating-layer delamination caused by high temperatures. Particularly, the damage in the edge region reveals that the tool surface was exposed to excessive thermal and mechanical loading during cutting [33]. According to the element maps in Figure 9b, it is seen that Ti and Cr elements belong to the coating layer and are concentrated in the upper parts of the surface. This shows that the coating was initially applied homogeneously but was locally deteriorated due to the effect of temperature during the process. It is observed that the C element is concentrated especially in the regions close to the cutting edge, which can be said to occur as a result of thermochemical reactions taking place under high temperatures. In addition, the high density of the W element in the edge regions indicates that the WCbased carbide structure in the lower layer is exposed as a result of the peeling of the coating layer. The distribution of the Fe element can be explained by the transfer of the workpiece material to the cutting surface by mechanical smearing or diffusion. These findings show that under dry cutting conditions, the coating layer is seriously damaged due to oxidation, diffusion, and adhesion-deterioration mechanisms, and this negatively affects tool life.

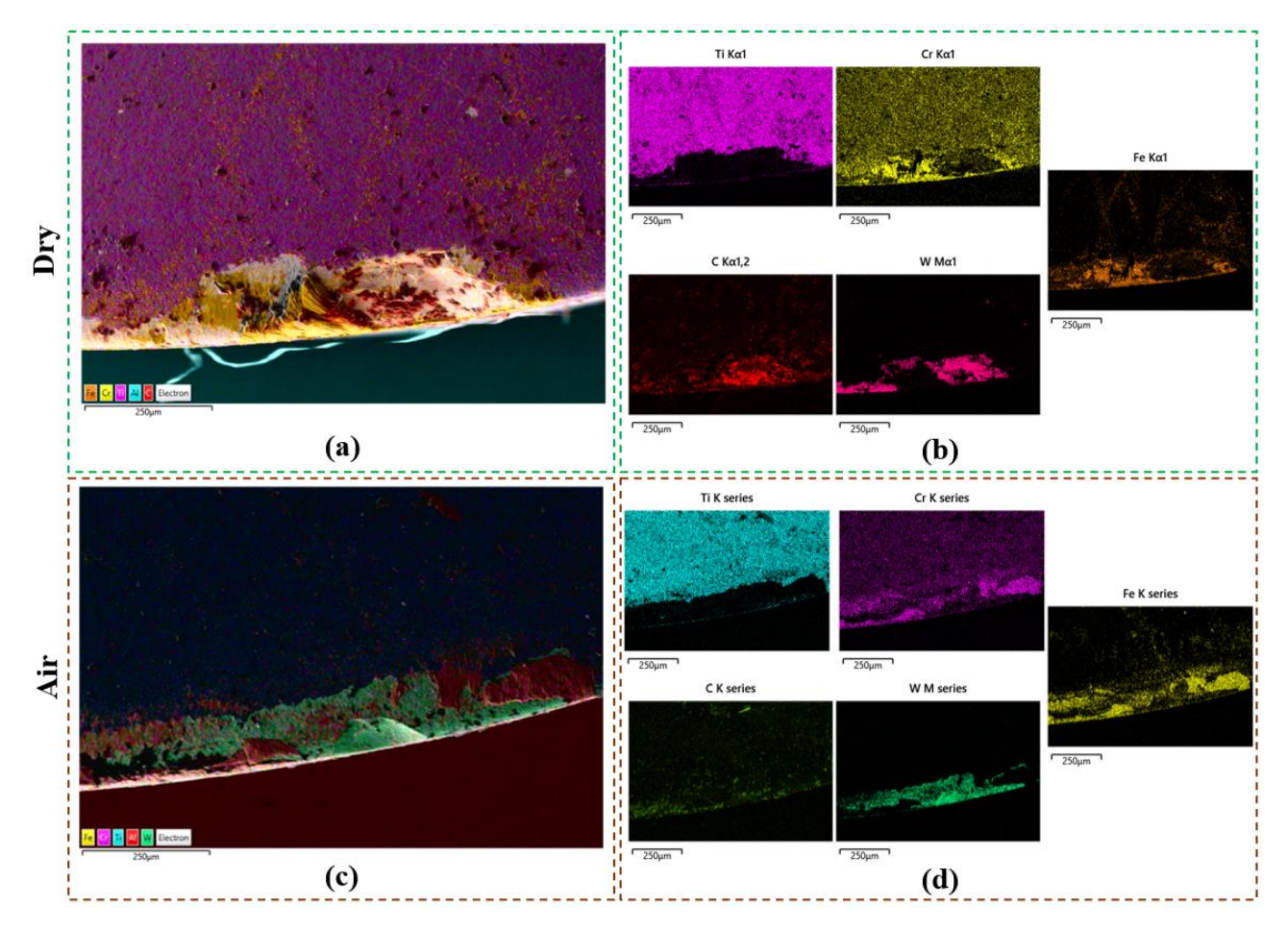


Figure 9. Layered images and element distribution of inserts (1500 rpm and 3000 mm/min).

When Figure 9c, obtained under air-assisted cutting conditions, is examined in detail, a much more balanced and smooth surface structure is observed compared to dry cutting. The fact that the coating layer is largely preserved indicates that the temperature increase is limited by the effective heat removal provided by the airflow in the cutting zone, and as a result, the coating integrity is preserved. The homogeneous distribution of Ti and Cr elements in the element maps in Figure 9d shows that the coating layer maintains its structural stability under air-assisted cooling. The distribution of the C element is less dense and more dispersed compared to dry cutting, indicating that cutting temperatures remain at lower levels and carbon accumulation is limited. Although the observation of the W element in the edge regions indicates limited coating peeling, the more balanced distribution density indicates that the substrate exposure is at a lower level. Generally speaking, under dry cutting conditions, serious damage occurs to the coating layer due to the effect of high temperatures; this situation, combined with thermochemical and mechanical effects, accelerates tool wear. Air-assisted cutting reduces the thermal load in the cutting zone, preserves the coating stability and the structural integrity of the tool, thus extending tool life [34]. The elemental maps clearly support the positive effects of this thermal control on the team.

Figure 10 presents the structural changes and elemental distributions that occur in the cutting inserts after the milling process performed at 2250 rpm and 4500 mm/min feed rate in a comparative manner under both dry and air-assisted cutting conditions. Figure 10a, obtained under dry cutting conditions, reveals that there are dense deposits and deteriorations in the coating layer, especially in the edge regions of the cutting edge. This observation shows that thermomechanical loads caused by high temperatures weaken the microstructural integrity of the coating layer, resulting in coating peeling and diffusion-related wear [34]. Indeed, according to the element maps in Figure 10b, the fact that Ti and Cr elements are distributed homogeneously on the upper surface of the coating confirms that the coating was initially applied properly, but this integrity was disrupted by the concentration of C, W, and Fe elements in the edge regions. Particularly, the high density of the C element around the cutting edge suggests that the high temperatures occurring during cutting trigger thermochemical reactions. The more pronounced concentration of the W element in the edge regions close to the surface can be associated with the exposure of WC-based carbide phases in the substrate with the coating peeling. Likewise, the presence of the Fe element in the contact areas of the cutting edge indicates that the

workpiece material is transferred to the tool surface by diffusion or mechanical smearing. These findings clearly reveal that diffusion, oxidation, and chemical reactions caused by high temperature in dry cutting conditions cause the coating layer to deteriorate and negatively affect tool life.

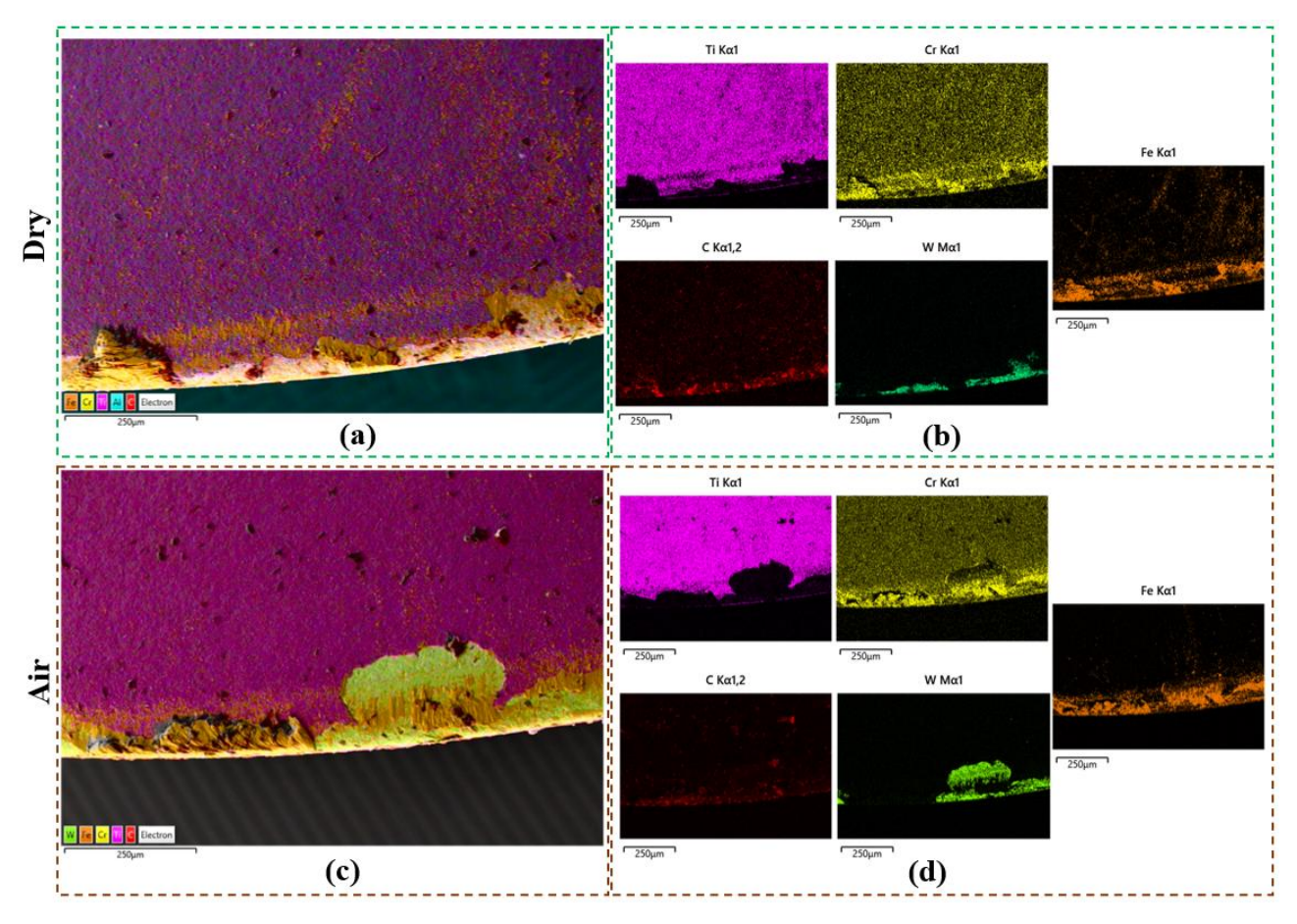


Figure 10. Layered images of inserts and element distribution (2250 rpm and 4500 mm/min).

On the other hand, when Figure 10c, obtained under air-assisted cutting conditions, is examined, the striking light-colored region is an area where the W element is locally enriched, indicating that the tungsten-based phases remaining under the layer separated from the coating are exposed. This indicates that there is limited degradation of the coating and that air cooling is limited at high cutting parameters. The elemental maps in Figure 10d confirm that the coating layer remains more thermally stable in air-assisted cutting. The more even distribution of Ti and Cr elements on the surface reveals that the coating is less affected by temperature-induced diffusion and deterioration. The limited carbon accumulation indicates that air cooling reduces the intensity of thermochemical reactions by lowering the temperature in the cutting zone. As a result, air-assisted cutting conditions limit substrate diffusion and adhesion-degradation mechanisms while preserving coating integrity [32]. This situation contributes to the delay of tool wear and the extension of tool life. The elemental mapping data obtained clearly supports the positive effects of air cooling on the tool-coating system.

The experimental studies comprehensively revealed the impacts of dry and air-assisted cutting mediums on T, Ra, and tool wear in face milling of AISI 316L stainless steel. It has been observed that air-assisted cooling significantly reduces cutting temperatures, makes temperature distribution more even, and improves surface quality, especially in this material that tends to have high heat accumulation. Additionally, SEM and EDS analyses show that air assist maintains coating integrity and can increase tool life by limiting the types of wear occurring on the tool surface. The findings show that air-assisted systems offer a more advantageous alternative compared to dry cutting in terms of preventing surface deterioration caused by high temperatures and wear.

4. CONCLUSIONS

The consequences of dry and air-assisted cutting environments on cutting temperature, surface roughness, and cutting tool wear during AISI 316L stainless steel machining using the HFM method were examined experimentally. The findings can be summarized as follows:

- ✓ The maximum cutting temperature recorded in dry machining was 321°C (at 1000 rpm and 4500 mm/min), while the same parameters in air-assisted cutting resulted in a significantly lower temperature of 197°C, corresponding to a 39% reduction. Under other parameter combinations, the air-assisted system maintained temperatures within a range of 162–221°C, whereas dry cutting often exceeded 280°C, indicating effective thermal control provided by airflow.
- ✓ The lowest Ra value under air-assisted cooling was 0.929 μm (at 1000 rpm and 2000 mm/min), while the highest was 1.414 μm. In contrast, dry cutting produced a higher Ra range between 1.100 μm and 1.654 μm, with the maximum value again occurring at 1000 rpm and 4500 mm/min.
- ✓ Surface roughness (Ra) values showed a generally lower and more balanced distribution under air-assisted milling conditions. This shows that better quality surfaces can be obtained by reducing thermal loads and keeping tool wear under control.
- ✓ Tool wear analyses (SEM and EDS) showed that significant coating peeling, material adhesion, and diffusion effects were observed in dry cutting, while tool surface integrity was largely preserved and adhesion effects were limited in air-assisted cutting. This shows that air-assisted cooling offers a significant advantage in terms of tool life.

In general, the air-assisted cooling system is an environmentally friendly, energy-efficient, and technically effective method that provides superiority over traditional dry machining methods in milling difficult-to-machine materials such as AISI 316L. In this context, it is recommended that air-assisted cooling systems be evaluated as a highly applicable and sustainable alternative in the industry to reduce tool wear and surface quality problems caused by high temperatures.

ACKNOWLEDGMENT

The authors thank Pars Defense & Aerospace for their support in conducting the experimental work.

REFERENCES

- [1] S. Debnath, M. M. Reddy, Q. S. Yi, Environmental friendly cutting fluids and cooling techniques in machining: A review, J Clean Prod 83 (2014) 33–47. doi: 10.1016/j.jclepro.2014.07.071
- [2] S. H. Ryu, D. K. Choi, C. N. Chu, Roughness and texture generation on end milled surfaces, Int J Mach Tools Manuf 46 (3–4) (2006) 404–412. doi: 10.1016/j.ijmachtools.2005.05.010
- [3] D. Biermann, P. Kersting, T. Surmann, A general approach to simulating workpiece vibrations during five-axis milling of turbine blades, CIRP Ann Manuf Technol 59(1) (2010) 125–128. doi: 10.1016/j.cirp.2010.03.057
- [4] R. Hense, C. Wels, P. Kersting, U. Vierzigmann, M. Löffler, D. Biermann, M. Merklein, High-feed milling of tailored surfaces for sheet-bulk metal forming tools, Prod Eng 9(2) (2015) 215–223. doi: 10.1007/s11740-014-0597-0
- [5] G. Uzun, R. Çakıroğlu, Investigation of Machinability Parameters in High-Feed Milling Process, Manuf Technol Appl 1(1) (2020) 34–41.
- [6] H. Dong, Z. C. Li, M. C. Somani, R. D. K. Misra, The significance of phase reversion-induced nanograined/ultrafine-grained (NG/UFG) structure on the strain hardening behavior and deformation mechanism in copper-bearing antimicrobial austenitic stainless steel, J Mech Behav Biomed Mater 119(2021) 104489. doi: 10.1016/j.jmbbm.2021.104489
- [7] A. Amininejad, R. Jamaati, S. J. Hosseinipour, Improvement of strength-ductility balance of SAE 304 stainless steel by asymmetric cross rolling, Mater Chem Phys 256 (2020) 123668. doi: 10.1016/j.matchemphys.2020.123668
- [8] B. Weiss, R. Stickler, Phase instabilities during high temperature exposure of 316 austenitic stainless steel, Met Trans 3(4) (1972) 851–866. doi: 10.1007/bf02647659
- [9] P. Kumar, R. Jayaraj, J. Suryawanshi, U. R. Satwik, J. McKinnell, U. Ramamurty, Fatigue strength of additively manufactured 316L austenitic stainless steel, Acta Mater 199 (2020) 225–239. doi: 10.1016/j.actamat.2020.08.033
- [10] N. Ahmed, I. Barsoum, G. Haidemenopoulos, R. K. A. Al-Rub, Process parameter selection and optimization of laser powder bed fusion for 316L stainless steel: A review, J Manuf Process 75 (2022) 415–434. doi: 10.1016/j.jmapro.2021.12.064
- [11] I. Korkut, M. Kasap, I. Ciftci, U. Seker, Determination of optimum cutting parameters during machining of AISI 304 austenitic stainless steel, Mater Des 25(4) (2004) 303–305. doi: 10.1016/j.matdes.2003.10.011
- [12] G. Özger, M. Akgün, H. Demir, Effect of sustainable cooling and lubrication method on the hole quality and machinability performance in drilling of AA7075 alloy with cryogenically treated carbide drills, Mater Test 67(5) (2025) 910-925.
- [13] R. Çakıroğlu, G. Uzun, Modeling of the Cutting Force and Workpiece Surface Roughness During the Milling Process with High Feed Using Artificial Neural Networks, Gazi J Eng Sci 7(1) (2021) 58–66. doi: 10.30855/gmbd.2021.01.07

- [14] D. Russo, G. Urbicain, A. J. Sánchez Egea, A. Simoncelli, D. Martinez Krahmer, Milling force model for asymmetric end-mills during high-feed milling on AISI-P20, Mater Manuf Process 36(15) (2021) 1761–1768. doi: 10.1080/10426914.2021.1944199
- [15] J. Duplák, M. Hatala, D. Dupláková, J. Steranka, Evaluation of time efficiency of high feed milling, TEM J 7(1) (2018) 13–18. doi: 10.18421/TEM71-02
- [16] G. Liu, B. Zou, C. Huang, X. Wang, J. Wang, Z. Liu, Tool damage and its effect on the machined surface roughness in high-speed face milling the 17-4PH stainless steel, Int J Adv Manuf Technol 83(1-4) (2016) 257-264. doi: 10.1007/s00170-015-7564-6
- [17] F. Jurina, T. Vopát, M. Kuruc, V. Šimna, The tool wear observation of milling tools in high feed machining of hardened steels, Ann DAAAM Proc 30(1) (2019) 753–757. doi: 10.2507/30th.daaam.proceedings.103
- [18] S. Ehsan, S. A. Khan, M. Rehman, Defect-free high-feed milling of Ti-6Al-4V alloy via a combination of cutting and wiper inserts, Int J Adv Manuf Technol 114(1–2) (2021) 641–653. doi: 10.1007/s00170-021-06875-0
- [19] M. Kuruc, M. Vozár, V. Šimna, T. Vopát, J. Moravčíková, J. Peterka, Comparison of high feed machining with conventional milling in terms of surfacequality and productivity, Ann DAAAM Proc 30(1) (2019) 376–383. doi: 10.2507/30th.daaam.proceedings.051
- [20] J. Xu, B. Rong, H. Z. Zhang, D. S.Wang, L. Li, Investigation of Cutting Force in High Feed Milling of Ti6Al4V, Mater Sci Forum 770 (2014) 106–109. doi: https://doi.org/10.4028/www.scientific.net/MSF.770.106
- [21] Y. Turgut, İ. Çakmak, Investigation of the Effect of Chip Breaker Form on Surface Roughness and Cutting Forces in AISI 1040 Steel Milling, Gazi Üniversitesi Fen Bilim Derg Part C Tasarım ve Teknol 7(2) (2019) 482–494 doi: 10.29109/gujsc.518229
- [22] D. López, N. A. Falleiros, A. P.Tschiptschin, ASTM A240 Standard Specification for Chromium and Chromium-Nickel Stainless Steel Plate, Sheet, and Strip for Pressure Vessels and for General Applications, ASTM 2004.
- [23] W. M. Chiang, F. J. Wang, Kusnandar, An experiment investigation of temperature control performance for machine tool oil coolers with hot-gas bypass temperature control scheme and inverter temperature control scheme, J Mech Sci Technol 35(2) (2021) 771–778. doi: 10.1007/s12206-021-0137-8
- [24] V. Y. Bhise, B. F. Jogi, Multi-response optimization and effect of process parameters during machining of inconel X-750 using grey relational analysis and analysis of variance, Int J Interact Des Manuf 19(6) (2024) 4073–4083. doi: 10.1007/s12008-024-01982-0
- [25] N. Tosun, C. Kuru, E. Altintaş, O. E. Erdin, Investigation of surface roughness in milling with air and conventional cooling method, J Fac Eng Archit Gazi Univ 25(1) (2010) 141–146.
- [26] Ü. Değirmenci, Nimonic-60 Süper Alaşımının Sürdürülebilir Koşullar Altında İşlenebilirlik Özelliklerinin Belirlenmesi, J Inst Sci Technol Üniversitesi Fen Bilim Enstitüsü Derg 14(3) (2024) 1228. doi: 10.21597/jist.1481108
- [27] J. Kundrák, A. P. Markopoulos, T. Makkai, I. Deszpoth, A. Nagy, Analysis of the effect of feed on chip size ratio and cutting forces in face milling for various cutting speeds, Manuf Technol 18(3) (2018) 431–438. doi: 10.21062/ujep/117.2018/a/1213-2489/MT/18/3/431
- [28] G. Yingfei, P. M. de Escalona, A. Galloway, Influence of cutting parameters and tool wear on the surface integrity of cobalt-based stellite 6 alloy when machined under a dry cutting environment, J Mater Eng Perform 26(1) (2017) 312–326. doi: 10.1007/s11665-016-2438-0
- [29] N. A. Abukhshim, P. T. Mativenga, M. A. Sheikh, Investigation of heat partition in high speed turning of high strength alloy steel, Int. J. Mach. Tools Manuf., 45(15) (2005) 1687–1695. doi: 10.1016/j.ijmachtools.2005.03.008.
- [30] J. Kundrak C. Felho, Topography of the machined surface in high performance face milling, Procedia CIRP 77 (2018) 340–343. doi: 10.1016/j.procir.2018.09.030
- [31] N. M. Liu, K. T. Chiang, C. M. Hung, Modeling and analyzing the effects of air-cooled turning on the machinability of Ti-6Al-4V titanium alloy using the cold air gun coolant system, Int J Adv Manuf Technol 67(5–8) (2013) 1053–1066. doi: 10.1007/s00170-012-4547-8
- [32] J. Nakagawa, Y. Yoshimi, K. Chiba, R. Tanaka, Evaluation and quantification of diffusion wear between cutting chip and workpiece using forging press, Manuf Lett 41 (2024) 588–594. doi: 10.1016/j.mfglet.2024.09.075
- [33] A. W. Nemetz, W. Daves, T. Klünsner, C. Praetzas, W. Liu, T.Teppernegg, J. Schäfer, Experimentally validated calculation of the cutting edge temperature during dry milling of Ti6Al4V, Journal of Mater Proces Techn 278 (2020) 116544. doi: 10.1016/j.jmatprotec.2019.116544
- [34] T. Obikawa, T. Ohno, R. Nakatsukasa, M. Hayashi, T. Tabata, High Speed Machining of Difficult-to-Machine Materials under Different Lubrication Conditions, Key Eng Mater 625 (2014) 60–65. doi: https://doi.org/10.4028/www.scientific.net/KEM.625.60
- [35] W. Wan, Q. Zhou, M. Liang, P.Wang, C. Rao, S. Ji, K. Fan, J. Song, Study on the high temperature wear behavior of TiAlSiN coatings deposited on WC-TaC-Co cemented carbides, Tribol Int 200 (2024) 110115. doi: 10.1016/j.triboint.2024.110115